

Design of multiphase carbon fiber reinforcement of crack existing concrete structures using topology optimization

Anh P. Nguyen^{1a}, Thanh T. Banh^{1b}, Dongkyu Lee^{*1}, Jaehong Lee^{1c}, Joowon Kang^{2d} and Soomi Shin^{3e}

¹ Department of Architectural Engineering, Sejong University, Seoul 05006, Korea

² Department of Architecture, Yeungnam University, Gyeongsan 38541, Korea

³ Research Institute of Industrial Technology, Pusan National University, Busan 46241, Korea

(Received August 8, 2018, Revised October 20, 2018, Accepted November 15, 2018)

Abstract. Beam-column joints play a significant role in static and dynamic performances of reinforced concrete frame structures. This study contributes a numerical approach of topologically optimal design of carbon fiber reinforced plastics (CFRP) to retrofit existing beam-column connections with crack patterns. In recent, CFRP is used commonly in the rehabilitation and strengthening of concrete members due to the remarkable properties, such as lightweight, anti-corrosion and simplicity to execute construction. With the target to provide an optimal CFRP configuration to effectively retrofit the beam-column connection under semi-failure situation such as given cracks, extended finite element method (X-FEM) is used by combining with multi-material topology optimization (MTO) as a mechanical description approach for strong discontinuity state to mechanically model cracked structures. The well founded mathematical formulation of topology optimization problem for cracked structures by using multiple materials is described in detail in this study. In addition, moved and regularized Heaviside functions (MRHF), that have the role of a filter in multiple materials case, is also considered. The numerical example results illustrated in two cases of beam-column joints with stationary cracks verify the validity, benefit and supremacy of the proposed method.

Keywords: CFRP; composite; multiple materials; topology optimization; X-FEM; MRHF; crack; beam-column joint

1. Introduction

In the last decades, the externally bonded carbon fiber-reinforced plastic is becoming popular means of repair and reinstatement to extend the service life of deterioration and distress structures. Carbon fibers are very fine fibers with a diameter of 9 to 17 μm and have excellent properties for structural members, for example, high strength, high elastic modulus, light weight, and high durability. Moreover, in comparison with other reinforced concrete (RC) structure repair techniques which involve replacing the existing element and external prestressing, adding the external reinforcement by CFRP is very attractive as it has little effect on the member dimensions as well as it can be applied directly while the structure is in use (Alonso *et al.* 2014, Alam 2014). From the 1980's, the application, as well as the study of CFRP materials to strengthen RC members, initiated in Japan and Switzerland by Kaiser (1989). And then, until the mid-1990's, the number of publications on journals and conference proceedings on this topic grew up

such as Beres *et al.* (1992), Gergely *et al.* (1998) along with Andra and Maier (1999). Recently, there are various studies about the utilization of CFRP on the reinforced concrete structure such as Kim *et al.* (2015). Song and Yu (2015) investigated beam, Abdel-Hafez *et al.* (2015) studied column, Anwar and Versailot (2016) surveyed frame structure and Amin *et al.* (2016) considered one-way slab. Moreover, many scientists tend to apply new technologies into CFRP domain as 3D printing (Zhou and Chen 2018, Hao *et al.* 2017) and fused deposition modelling (FDM) method (Gavali and Kulkarni 2018). By applying computational formulation based on isogeometric analysis (IGA), there are many researches contributing for carbon nano-reinforced composite structure in various situation such as Phung *et al.* (2015, 2017a, b, 2018) and Le *et al.* (2018). Besides, the vibrations along with both dynamic and static topics of this kind of composite structure are also investigated by Nguyen *et al.* (Nguyen and Do 2013, Nguyen *et al.* 2017a, b), Nguyen and Do (2014), Pham and Nguyen (2016), and Nguyen and Pham (2017c).

Recent earthquakes over the world have pointed out the vulnerability of existing reinforced concrete beam-column joints to seismic loading as Maria (2016). Poorly detailed joints, especially exterior ones, have been identified as critical structural elements, which appear to fail prematurely, thus performing as "weak links" in reinforcement concrete frames (Truong and Choi 2017). When subjected to lateral forces, the beam-column joint is prone to joint shear failure due to high shear stress which

*Corresponding author, Associate Professor,
E-mail: dongkyulee@sejong.ac.kr

^a M.Sc. Student

^b Ph.D. Student

^c Professor

^d Professor

^e Research Professor

appears in the joint panel as a result of opposite sign moments on both sides of the joint core. Especially here, the model of beam-column connection is considered in a dangerous situation, when suffering from lateral load and having crack patterns at the corner. Besides, the presence of cracks in structure is a popular issue and also attracted by some researchers (Doan *et al.* 2017, Pham *et al.* 2018). In this study, a motivation of considering crack patterns comes from the fact that people usually retrofit the structure only when it appears the visible signal of the harm such as cracks.

Structural topology optimization is a computational technique which has been studied by many researchers all over the world for many decades for distributing material efficiently across a design domain in order to both improve stiffness and reduce mass in the resulting design. It has been found its way into industry and is used in a variety of engineering fields such as economics, biology, electronics, aerospace, civil and building construction, etc. Due to significant advantages in topology optimization, it has been developed for different problems such as multi-joint (Woischwill and Kim 2018), plate structures (Banh and Lee 2018a, b, Lieu *et al.* 2018a, b), multi-phase architected materials (Asadpoure *et al.* 2017, Lieu and Lee 2017), laminated composite structures (Blasques and Stolpe 2012), thermoelastic structures (Xia and Wang 2008), buckling problem (Doan and Lee 2017), fundamental compliant mechanisms (Shahri and Moeenfard 2018), and cracked structures (Shobeiri 2015, Banh and Lee 2018c).

To discover the multi-material design distribution, the alternating active phase algorithm of optimal criteria introduced by Tavakoli and Mohseni (2014) is used. The multi-material-phase field approach is based on the Cahn-Hilliard equation, and a general method to solve multi-phase structure topology optimization problems was presented by Zhou and Wang (2006). However, these studies dealt with continuum structures with a continuous displacement field. A numerical approach to optimize topologies for structures with the presence of cracks by using multiple materials (Banh and Lee 2018c) is employed. In addition, in this study, moved and regularized Heaviside functions (MRHF) are first implemented for filtering of multi-material topology optimization with cracked structures, and then the present results are compared with the general those in cases of multiple materials.

This research aims to find the most effective arrangement of CFRP for retrofitting the beam-column connection with existing initial cracks, while using computational procedures of multi-material topology optimization of a continuum structure with a discontinuous displacement field. CFRP is an expensive material. It is more costly material than its counterparts in the construction industry including glass fiber-reinforced polymer (GFRP) and aramid fiber-reinforced polymer (AFRP), thanks to having superior properties. Therefore, instead of fully material wrapping for the component, the resulting configuration arrangements obtained from topology optimization identify the most significant and appropriate reinforced area of CFRP of the surveyed

structure. It is expected to be beneficial in terms of structure shear capacity, overall connection damage tolerance, and economic aspects. Furthermore, a moved and regularized Heaviside functions filter, which affects the obvious topology results by especially using multiple materials in terms of the existence of the physical material, is also considered. The results obtained from the single material and multi-material topology optimization procedures are then compared and discussed in this paper.

The contents of this study are organized as follows. This study begins in Section 2 with a brief of carbon fiber reinforced plastic in the field of construction. The analysis models of multi-material topology problem for cracked structures including MRHF formulations for multiple materials, stiffness formulation and sensitivity analysis of compliance for structures are detailed in Section 3. As numerical examples, the resulting configuration arrangement of beam-column connection for CFRP is discussed in Section 4. Finally, conclusions are drawn in Section 5.

2. Carbon Fiber Reinforced Plastic (CFRP)

A fiber reinforced polymer (FRP) is a linear elastic composite material that consists of a polymer matrix reinforced with a fibrous material. Three types of fiber are widely used in the construction of FRPs: aramid, glass and carbon. All three have higher ultimate strengths than normal reinforcing steel (Masuelli 2013). In this study, carbon fiber is considered due to many uses in the construction industry. The polymer is usually an epoxy, a vinyl ester or a polyester thermosetting plastic, and phenol formaldehyde resins are still in use. FRPs are commonly used in the aerospace, automotive, marine, and construction industries.

Carbon fiber reinforced plastic is a very strong and light fiber-reinforced polymer which contains carbon fibers. Carbon fibers are created, when polyacrylonitrile fibers (PAN), Pitch resins, or Rayon are carbonized (through oxidation and thermal pyrolysis) at high temperatures. Based on modulus, strength, carbon fibers can be classified into five categories including ultra-high modulus (over 450 GPa); high modulus (between 350 and 450 GPa); intermediate modulus, (between 200 and 350 GPa); low modulus and high tensile (below 100 GPa and tensile strength over 3.0 GPa); super high tensile (strength over 4.5 GPa), here $1 \text{ GPa} = 1000 \text{ MPa} = 100000 \text{ N/cm}^2$.

Existing capacity and calculated deficiency of the specific structural elements must be considered in order to correctly place and structurally retrofit actual structures. Strengthening of CFRP should be considered as secondary to existing reinforcement. Therefore, the placement onto properly prepared surfaces is one of the most important steps when applying CFRP products. Surface preparation should be in accordance with ACI-546R and ICRI-0370 (American Concrete Institute 2004, International Concrete Repair Institute 2008). Epoxy primers designed to penetrate the substrate and epoxy putty applied to fill small anomalies, provide the bonding adhesive for carbon fabric and strips. Using the modified "dry method" described in ACI-440, the first layer of fabric or strip is applied with the

CFRP surface rolled and squeegeed to remove air.

In addition to the existing standards for designing and assembling CFRP, in this study, topology optimization is applied to fiber reinforced composites. To distribute a limited amount of fiber reinforcement, a problem of topology optimization is formulated to simultaneously search for the optimal regions to be strengthened. Moreover, the concept of multiple materials in topology optimization is applied in this case due to the possibility of using multiple reinforced material. Based on the elastic modulus, three types of CFRP is considered in models to discover the optimal layout for each kind of material.

3. Topology optimization model for multiple materials

To date, many approaches have been developed and proposed for solving topology optimization problems. Since the pioneering study by Bendsøe and Kikuchi (1988), topology optimization has made remarkable progress as an innovative numerical and design method, drawing an enormous amount of attention from the scientific community. Multi-material topology optimization is also an attractive issue in the field of structural topology optimization. In addition to inherit of main ideas of standard topology optimization, the optimal material distribution of variable densities is continuously derived. By using more additional stiff materials, topology optimization may produce structures with higher stiffness. It also offers material cost savings in compared with single material structures to arrive at required design performance.

3.1 Multi-material interpolation

The minimum compliance based on topology optimization problem for multiple materials within an available design domain Ω discretized by quadrilateral isoparametric finite element is considered. Domain schematic design of multi-material topology optimization is divided and subdomains is shown in Fig. 1, where Ω_{void}^j ($j = 1, 2, \dots, n$) is void material of domain. Ω_s^m and Ω_v^m are the solid domain of material and void domain in a multi-material problem, respectively. Each design variable is now represented by the density vector α containing elemental densities α . Relative densities of each element are design variables α connected into a vector α . Following Bendsøe and Sigmund (1999), void is considered as a separate material phase, the multi-material topology optimization to find the optimal material distribution of n number of materials corresponding to find $n+1$ material phases $\alpha_i = \alpha_i(x)$ at each point $x \in \Omega$. The local stiffness tensor E based on the modified SIMP version of linear interpolation for multiple materials can be formulated by incorporating alpha as an integer formulation

$$E(\alpha) = \sum_{i=1}^{n+1} \alpha_i^p E_i^0 \quad (1)$$

where p is the penalizing factor that penalizes elements with

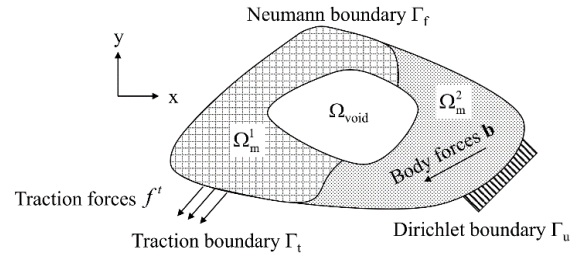


Fig. 1 A design domain schematic for multi-material topology optimization

intermediate densities to approach 0 or 1. Thus, the penalization is achieved without introducing any explicit penalization scheme. For materials with Poisson's ratio $\nu = 0.3$, it is recommended in Bendsøe and Sigmund (1999) to use $p \geq 3$. E_i^0 is elastic modulus corresponding to phase i -th.

3.2 Moved and regularized Heaviside functions for multi-phase topology optimization problem

According to alternating active phase algorithm proposed by Tavakoli and Mohseni (2014), the multi-phase topology optimization problem is solved by converting the multi-phase into $n(n+1)/2$ binary phases sub-problem. Each binary sub-problem is a so-called active phase. This solver could be made by modification of the binary phase topology optimization algorithm. In this process of each sub-problem, only two phases denoted as 'a' and 'b' are active at a time and the other phases are fixed. The problem can be simplified in each binary phase topology optimization subproblem in each computational step by taking the density of active phase 'a' as the only design variable. Overlaps are not allowed in a desired optimal design, thus summation of the densities at each point $x \in \Omega$ should be equal to unity. In other words, the density summation of two active phases at each point $x \in \Omega$ can be calculated as follows

$$\alpha_a(x) + \alpha_b(x) = 1 - \sum_{i=1, i \neq \{a,b\}}^{n+1} \alpha_i(x) = r \quad (2)$$

Moved and regularized Heaviside functions (MRHF) are discontinuous functions, whose values are toward zero for below 0.5 argument and toward one for above 0.5 argument. The MRHF acts as a filter of density of elements in the design domain which have values close to zero and one. Within the scope of this study, MRHF is also considered as a filter variable density of elements for each binary phase in the design domain. Four MRHF equations that based on the proposal of Lee and Shin (2015) can be written to framework of multi-material topology optimization problem as follows

$$\alpha_a^{MRHF(1)} = \frac{3}{4} \left[\frac{\alpha_a - 0.5r}{\rho} - \frac{r}{3} \left(\frac{\alpha_a - 0.5r}{\rho r} \right)^3 \right] + \frac{r}{2} \quad (3a)$$

$$\alpha_a^{MRHF(2)} = \frac{r}{2} + \frac{2r}{\pi} \arctan \left(\frac{\alpha_a - 0.5r}{\rho r} \right) \quad (3b)$$

$$\alpha_a^{\text{MRHF}(3)} = \frac{r}{2} \left[1 - \frac{\alpha_a - 0.5r}{\rho r} - \frac{1}{\pi} \sin \left(\frac{\pi(\alpha_a - 0.5r)}{\rho r} \right) \right] \quad (3c)$$

$$\alpha_a^{\text{MRHF}(4)} = \frac{r}{2} \left[1 + \sin \left(\frac{\pi(\alpha_a - 0.5r)}{2\rho r} \right) \right] \quad (3d)$$

where ρ is considered to 0.5. Note that the range of α_a within each sub-problem is now in the range of 0 to r (Fig. 2), here the parameter r is defined in Eq. (2). Then, the density of phase ‘ b ’ (or background phase) can be calculated through the density of corresponding phase ‘ α_a^{MRHF} ’, by using Eq. (2).

3.3 Multi-material topology optimization problem formulation for cracked structures

To avoid singularities in computational calculation processes of topology optimization, the problem is relaxed for densities between 0 and 1 by a very small lower bound non-zero value ε_i . The general mathematical formulation of structural multi-material topology optimization problem for cracked structures can be stated as follows

$$\begin{aligned} & \underset{\alpha}{\text{minimize}} : C(\alpha_i, \mathbf{U}) = \mathbf{U}^T \mathbf{K} \mathbf{U} \\ & \text{subject to} : \mathbf{K}(\alpha) \mathbf{U} = \mathbf{F} \\ & \int_{\Omega} \alpha_i dx \leq V_i \\ & 0 < \varepsilon_i \leq \alpha_i \leq 1 \end{aligned} \quad (4)$$

where C is structural compliance. α_i is the density vector for phase material i -th. V_i is the per-material volume fraction constraint with $i = 1 : n+1$ such that the summation should be equal to unity $\sum_i V_i = 1$. The global stiffness matrix \mathbf{K} , global load vector \mathbf{F} and global displacement vector which collects the displacement control variables and additional

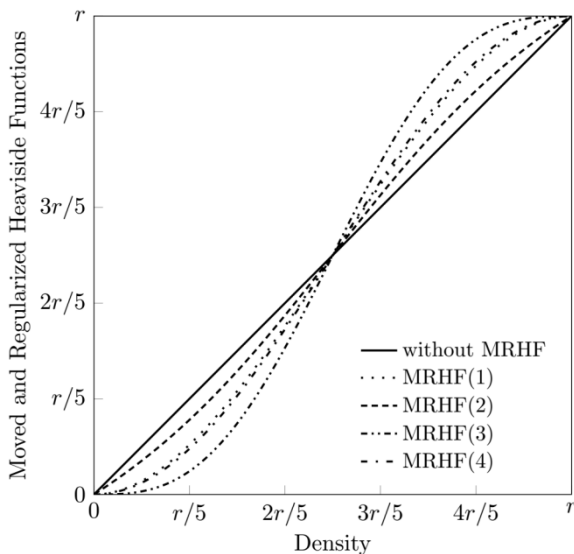


Fig. 2 Moved and regularized Heaviside functions (MRHF) in each binary phase sub-problem

enrichment degrees of freedom \mathbf{U} can be written as follows in turn.

$$\mathbf{K}_{ij}^e = \int_{\Omega^e} \begin{bmatrix} \mathbf{B}_i^{uT} \bar{\mathbf{D}} \mathbf{B}_j^u & \mathbf{B}_i^{uT} \bar{\mathbf{D}} \mathbf{B}_j^a & \mathbf{B}_i^{uT} \bar{\mathbf{D}} \mathbf{B}_j^b \\ \mathbf{B}_i^{aT} \bar{\mathbf{D}} \mathbf{B}_j^u & \mathbf{B}_i^{aT} \bar{\mathbf{D}} \mathbf{B}_j^a & \mathbf{B}_i^{aT} \bar{\mathbf{D}} \mathbf{B}_j^b \\ \mathbf{B}_i^{bT} \bar{\mathbf{D}} \mathbf{B}_j^u & \mathbf{B}_i^{bT} \bar{\mathbf{D}} \mathbf{B}_j^a & \mathbf{B}_i^{bT} \bar{\mathbf{D}} \mathbf{B}_j^b \end{bmatrix} d\Omega \quad (5a)$$

$$\mathbf{F}_i = \left\{ \mathbf{F}_i^u \quad \mathbf{F}_i^a \quad \left\{ \mathbf{F}_i^{b_j} \right\}_{j=1,4} \right\} \quad (5b)$$

$$\mathbf{U} = \left\{ \mathbf{u} \quad \mathbf{a} \quad \left\{ \mathbf{b}_j \right\}_{j=1,4} \right\} \quad (5c)$$

where $\bar{\mathbf{D}} = \sum_{k=1}^{n+1} \alpha_k^p D_k^0$ with D_k^0 is the material property matrix corresponding to the phase material, k -th, including Poisson's ratio ν and nominal elastic modulus E_k^0 .

$$\mathbf{D}_k^0 = \frac{E_k^0}{1-\nu^2} \begin{bmatrix} 1 & \nu & 0 \\ \nu & 1 & 0 \\ 0 & 0 & (1-\nu)/2 \end{bmatrix} \quad (6)$$

where \mathbf{B}_i^u is standard strain–displacement matrix with $(\mathbf{B}_i^\xi)_{\xi=a,b}$ enriched part as follows

$$\mathbf{B}_i^u = \begin{bmatrix} N_{i,x_1} & 0 \\ 0 & N_{i,x_2} \\ N_{i,x_2} & N_{i,x_1} \end{bmatrix} \quad (7a)$$

$$\mathbf{B}_i^a = \begin{bmatrix} N_{i,x_1} \xi_i + N_i \xi_{i,x_1} & 0 \\ 0 & N_{i,x_2} \xi_i + N_i \xi_{i,x_2} \\ N_{i,x_2} \xi_i + N_i \xi_{i,x_2} & N_{i,x_1} \xi_i + N_i \xi_{i,x_1} \end{bmatrix} \quad (7b)$$

where ξ_i can represent either Heaviside function H or basis functions of the asymptotic solution $\{\psi^\beta\}_{\beta=\overline{1,A}} = \sqrt{r} \left\{ \sin \frac{\theta}{2}, \cos \frac{\theta}{2}, \sin \theta \sin \frac{\theta}{2}, \sin \theta \cos \frac{\theta}{2} \right\}$.

3.4 Discrete sensitivity formulation

The discrete sensitivities of objective function C in terms of multi-material densities for multi-material topology optimization can be written as follows

$$\frac{\partial C}{\partial \alpha_a^e} = -\mathbf{U}_e^T \frac{\partial \mathbf{K}^e}{\partial \alpha_a^e} \mathbf{U}_e \quad (8)$$

where the sensitivity matrix components of each elemental stiffness for multi-material formulation in terms of design variable of phase ‘ a ’ is expressed as follows

$$\frac{\partial \mathbf{K}_{ij}^{rs}}{\partial \alpha_a^e} = p \alpha_a^{p-1} \int_{\Omega^e} \mathbf{B}_i^{rT} (\mathbf{D}_a^0 - \mathbf{D}_b^0) \mathbf{B}_j^s d\Omega \quad (9)$$

with $r, s = u, a, b$. U_e and α_a^e are the displacement vector and density of phase 'a' of e -th element, respectively.

In computational field of topology optimization, the sensitivity filter is a technical part that not only ensure existence of solutions to topology optimization problem and to avoid the formation of checkerboard patterns, but also take highly beneficial when searching for a mesh independent solution whilst not adding on to much computational time or any extra constraints (Bendsøe and Sigmund 2004).

The filter scheme modifies the element sensitivities with respect to the objective function are expressed as follows

$$\frac{\partial C^{new}}{\partial \alpha_a^e} = \frac{\sum_i \tilde{H}_{ei} \alpha_{ai}^e (\partial C / \partial \alpha_a^e)}{\alpha_a^e \sum_i \tilde{H}_{ei} \alpha_{ai}^e} \quad (10)$$

where the convolution operator \tilde{H} is based on the distance to neighborhood elements as $\tilde{H}_{ei} = r_{min} - dist(e, \{f \in N | dist(e, f) \leq r_{min}\})$. As shown in Fig. 3, $dist(e, f)$ is the distance between the center of the considered element f and the neighborhood element e . The neighborhood elements are defined within a circle with the filter radius r_{min} . This filter has a role as the physical length scale which is independent on the discretization mesh, as shown in Fig. 3.

4. Numerical examples

In this section, models of beam-column joint with stationary cracks under a lateral impact load in two cases dividing based on the position of external connection in the concrete frame are considered as shown in Fig. 4. Each node has horizontal and vertical degrees of freedom, which

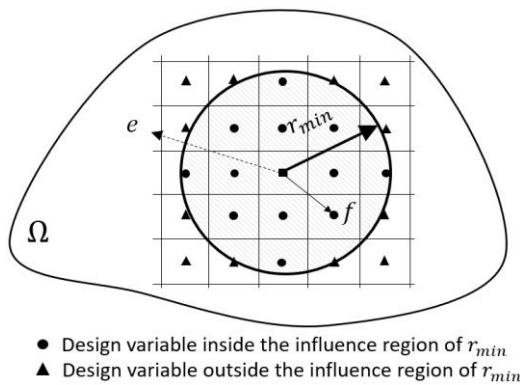


Fig. 3 Radius filter r_{min} and its influence region

can be imposed with loads and/or restrained to create boundary conditions. In all examples, Poisson's ratio of CFRP is chosen to be 0.3. Filter radius r_{min} is set equal to 3.0, and the parameter penalization for interpolating elasticity properties of 3.0 is used. According to the material properties in Section 2, this study considers CFRP with the intermediate modulus ($E^0 = 200$ GPa) and ultra-high modulus ($E^0 = 600, 1800, 2400$ GPa). The four types of CFRPs have a huge difference in the modulus to observe clearly the impact of the multi-material on topology optimization. The material properties of the structures are given in Table 1, wherein the indicators r, b, g and y denote red, blue, green and yellow colors, respectively. Note that Young's modulus and volume fraction of void material are selected $E = 10$ and $V_v = 1 - \sum_{k \neq v} V_k$ for all examples. The total volume fraction is fixed to be 50% during every optimization iteration.

4.1 Case 1: L-lateral exterior joint

In first case, the non-scaled design domain is modeled as a lateral -L-shape with the length $L(40)$ and the width $H(30)$, as shown in Fig. 5. The optimized results are surveyed for one, two and three various materials. The design domain is discretized by 3168 finite elements. As the input data, the length of crack $l_c = 4.15$, the magnitude of force $F = 200$ and the angle of crack $\theta = 75^\circ$ are used.

All detailed optimal topologies results for one to three various material of case 1 are presented in Figs. 6, 8 and 10, respectively. The multi-materials volume sensitivity filter (MVSF) that is the filtering method in the study of Banh and Lee (2018c) is also investigated in this paper for verification. The surveys point out the reliability of using MRHF through the similar results in both filters. Moreover,

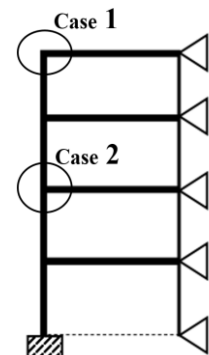


Fig. 4 Target joints in concrete frame

Table 1 Multi-material properties

Material properties	Number of materials			
	(a) One	(b) Two	(c) Three	(d) Four
Young's modulus	$E_r^0 = 2e5$	$E_r^0 = 2e5,$ $E_b^0 = 6e5$	$E_r^0 = 2e5, E_b^0 = 6e5$ $E_g^0 = 18e5$	$E_r^0 = 2e5, E_b^0 = 6e5$ $E_g^0 = 18e5, E_y^0 = 24e5$
Volume fraction (50%)	$V_r = 50\%$	$V_r = 30\%,$ $V_b = 20\%$	$V_r = 25\%, V_b = 15\%$ $V_g = 10\%$	$V_r = 20\%, V_b = 15\%$ $V_g = 10\%, V_y = 5\%$

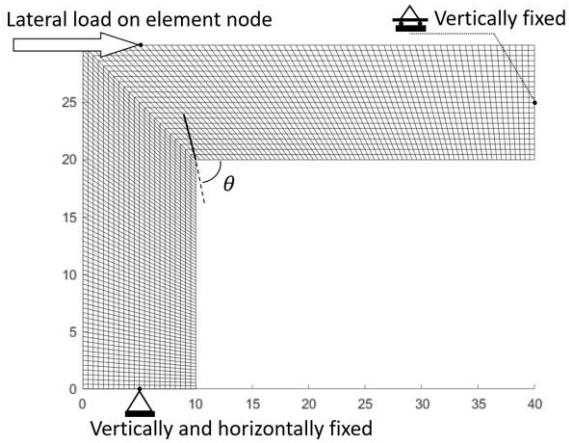


Fig. 5 Case 1: L-type exterior joint

optimized structure model tends to be more suitable with MRHF than MVSF. Indeed, in Fig. 6, MRHF(1) and MRHF(4) give more smooth and stiff results than MVSF. Especially, MRHF(1) and MRHF(4) provide more clear configuration in cases of multiple materials as in Figs. 8 and 10. Among them, MRHF(2) produces the least change of compliance and MRHF(3) results in the most change, in comparisons with the material distribution of the result without MRHF. MRHF(1) and (4) tend to be more stable and better than other cases in terms of convergence and

optimal topology. MRHF(2) tends to be close to the standard convergence line (without MRHF) and MRHF(3) takes more curved lines than the other lines. It shows that optimal topologies are not only varied depending on the number of material, but also depending on filters with the MRHF. They exhibit a major change in compared to the standard ones. Furthermore, the converged compliance

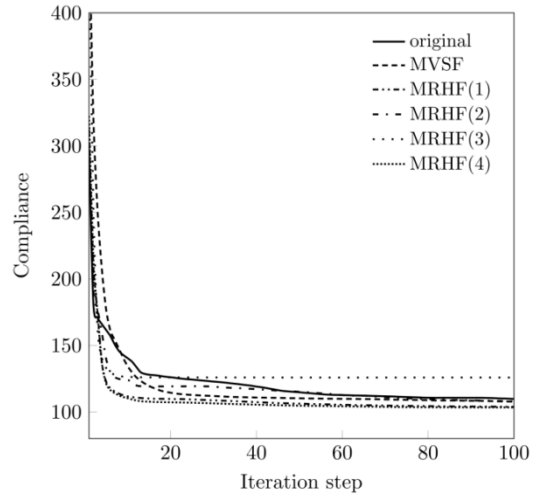


Fig. 7 Convergence histories of objective functions of single material in case 1

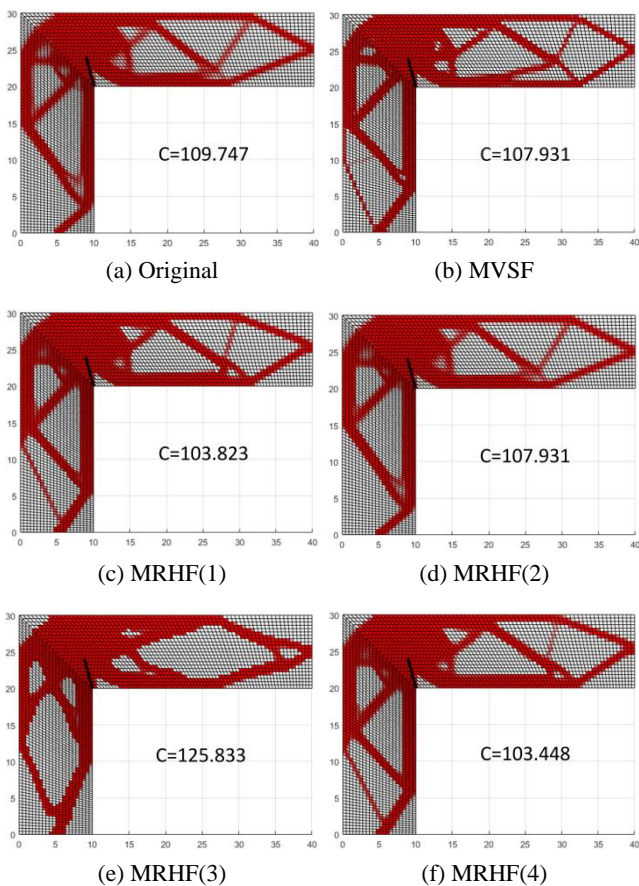


Fig. 6 Distribution of material densities by using single material according to different filters

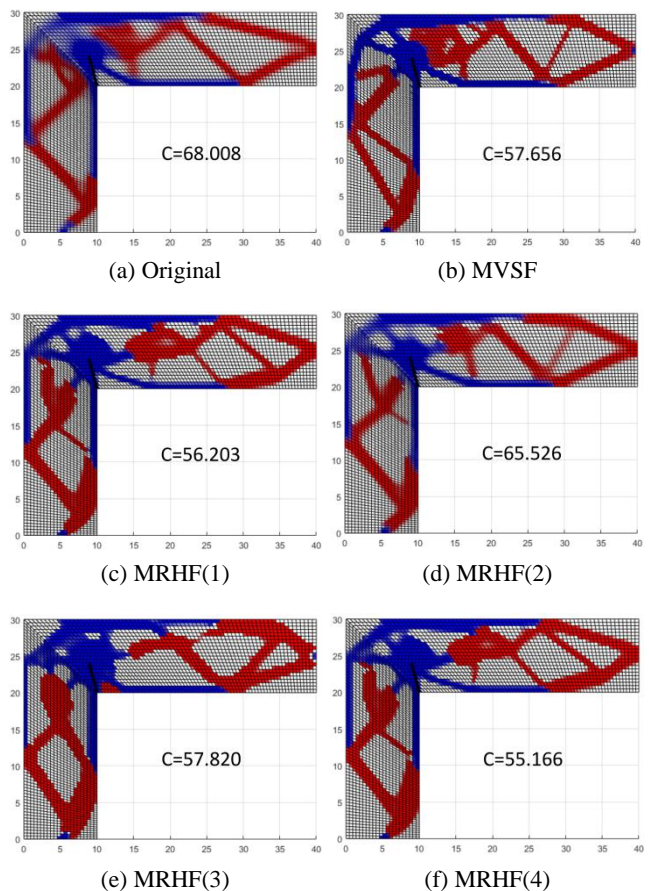


Fig. 8 Distribution of material densities by using two materials according to different filters

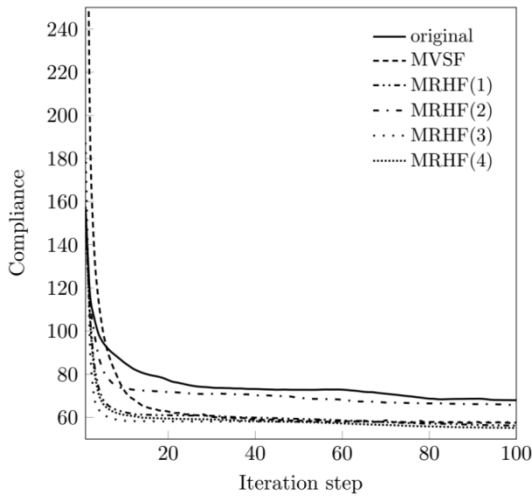


Fig. 9 Convergence histories of objective functions of two materials in case 1

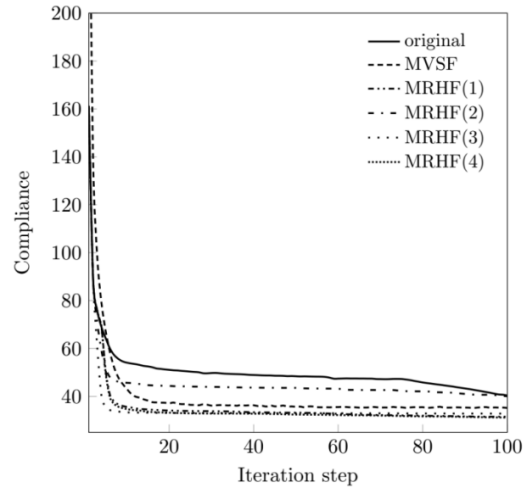


Fig. 11 Convergence histories of objective functions of three materials in case 1

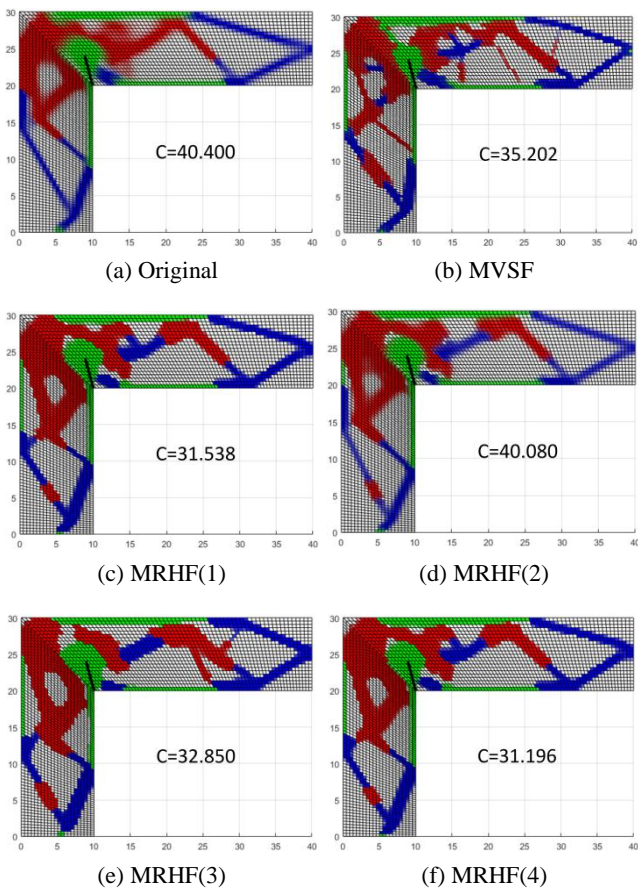


Fig. 10 Distribution of material densities by using three materials according to different filters

values with MRFH filter tend to be smaller than that without MRHF, as shown in Figs. 7, 9 and 11. Especially, in case of MRHF(4), the material density distribution is more stable and yields faster convergence than the rest ones. Hence, MRHF significantly affects the topology results, especially in the multi-material topology optimization problem.

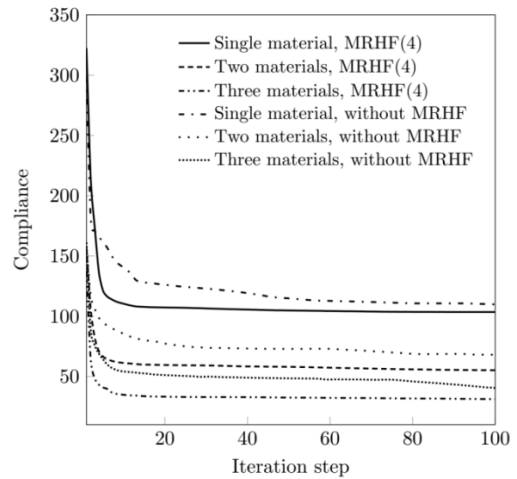


Fig. 12 Convergence histories of objective functions between with MRHF(4) and without MRHF

In the next examples, MRHF(4) filter is used to get the best optimal topology results. The benefit of MRHF(4) compares with original ones (without MRHF) within three kinds of materials is shown in Fig. 12.

This numerical example also aims to investigate the effect of crack angle affecting the distribution of material and the compliance in topology optimization. Fig. 13 shows the influence of various angle of crack patterns $\theta = \{0^\circ, 15^\circ, 30^\circ, 45^\circ, 60^\circ, 75^\circ, 90^\circ\}$ on optimized topologies design through MRHF(4) filter by using three various materials types. As the results, the values of compliance in seven situations express the quadratic curve that reaches the peak at the angle of 45 degrees. In general, with whatever angle of crack as well as any type of MRHF, it can be seen that the distribution of material emphasizes areas around the cracks, especially near the top of the crack. Indeed, a big quantity of material and stiff materials settled at the head of crack tend to prevent the extension of crack pattern. Besides, results showed that edges along the beam and column should be also well retrofitted according to the stiffest material distribution.

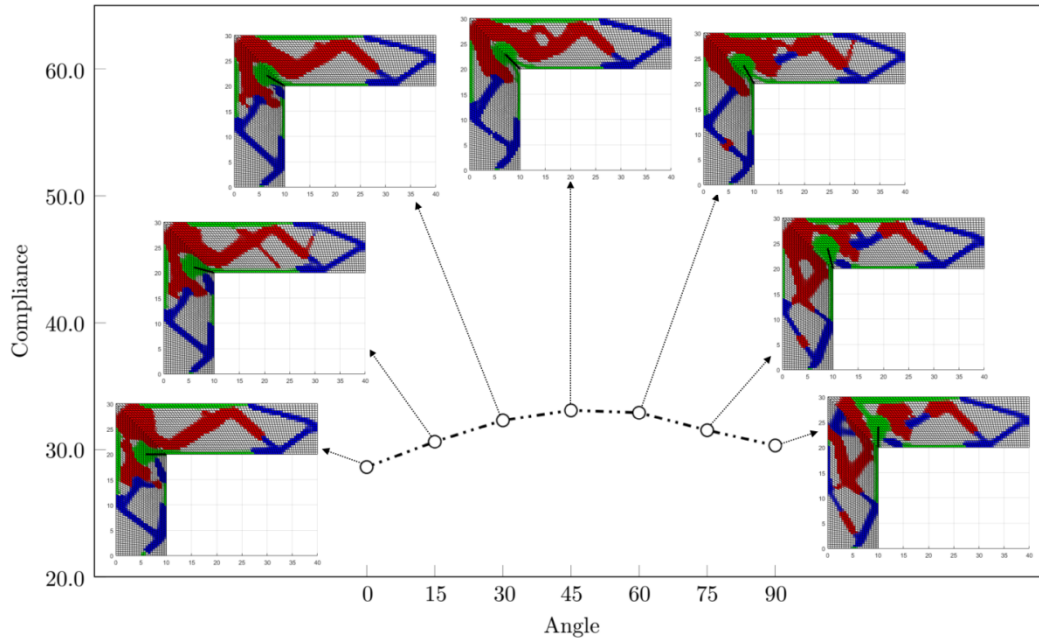


Fig. 13 The effects of crack angle for optimized topologies design with three materials and MRHF(4) filter

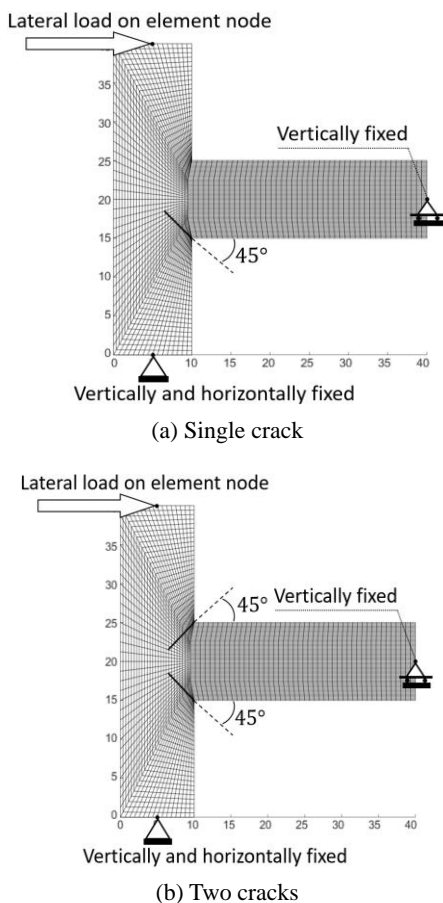


Fig. 14 Case 2: T-lateral exterior joint

4.2 Case 2: T-lateral exterior joint

In this case, the design domain is modeled as horizontal T-shape with geometric dimensions, load position and

boundary conditions as shown in Fig. 14. In this example, two given crack pattern cases are considered: a single crack and two symmetrical cracks. Based on the example of previous L-type exterior joint, the cracks angle of 45 degrees is chosen for the model to survey the distribution of multi-material. Actually, when considering concrete material, the diagonal shear crack with the angle of 45 degrees is the most popular and dangerous signal of structure. Four cases various materials by using multi-material topology optimization through MRHF(4) are investigated. The design domain is discretized by 4608 finite elements. As the input data, the length of each crack $l_c = 5$ and the magnitude of force $F=200$ are used.

The results in Fig. 15 highlight the change in compliance values due to adjusting the number of materials and cracks in the surveyed model. Clearly, the multi-material usage in optimization may provide the smallest converged compliance substantially. Particularly, the value of compliance in case of four materials is four-time lower in comparisons with that of single material. In contrast, adding one more crack pattern may lead to higher risk for the structure, as can be seen by the predominant value of compliance of the models having two cracks. Moreover, the converged compliance by applying multi-material tends to be smaller than that by only one material in both one and two cracks patterns, as shown in Fig. 16. Similar to the first example, stiffer material, as well as larger area of material, mostly reside in the region around cracks.

Through the geometrical distribution of material density, the results may be considered as the shape of CFRP strips and sheets. For an ideal distribution, four kinds of carbon fiber locating on the frame as results of this study propose the optimal retrofitted structure of bearing capacity as well as saving material. However, it is hard to state that those topology optimization results become applied directly in real life for bonding CFRP. This study highlights the most significant areas in the beam-column joint that needs to take

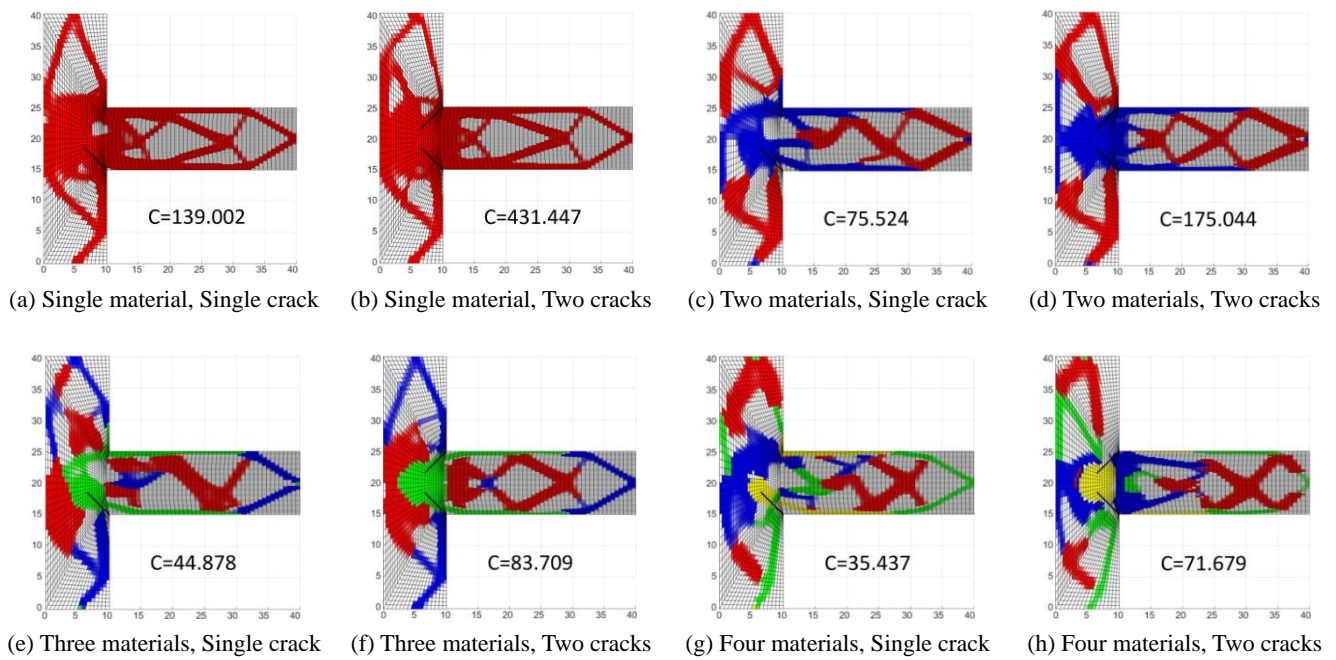


Fig. 15 Distribution of material densities of case 2 by using one to four materials and MRHF(4) filter

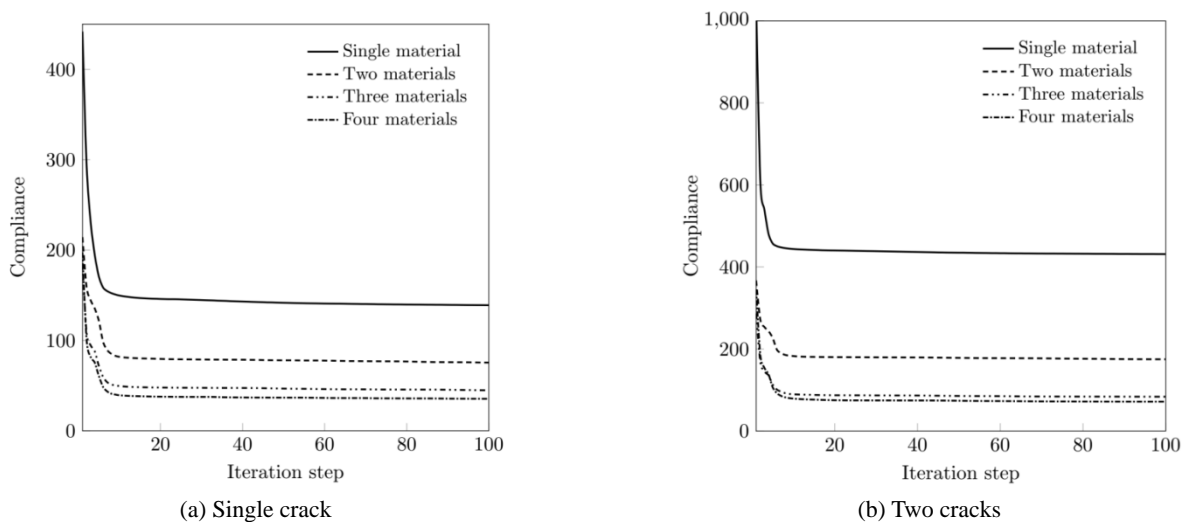


Fig. 16 Convergence histories of objective functions in both cases of single and two cracks using MRHF(4)

careful attention when designing and carrying out to retrofit through CFRP. Indeed, finding out regions that mostly absorption energy is the prerequisite work to improve ductility and longevity of a structure. For examples of a real application, as a serious drawback of retrofitting by CFRP, the intolerance to uneven bonding surfaces may cause peeling of the plate away from the concrete surface. To avoid the risk, based on material area obtained by computation of topology optimization procedure, those surfaces should be prepared excellently as well as special glue to bond.

5. Conclusions

This paper proposes topology optimization computation

of multi-materials CFRP for retrofitting the concrete beam-column joint with various cases of crack patterns. By finding out the vital area bearing force, the achieved results may inspire to improve the performance and endurance as well as the economic problem of external CFRP retrofit. In all example, the complex material strips located at the inner part of the beam and column of the structure are simulated for the real CFRP sheets. Especially, edges along the beam and column together with the area around crack are pointed out as the regions requiring the most significant reinforcement. Moreover, in case multi-material CFRP, the benefit and advantage of using MRHF filter are also generated in the present study. Numerical applications are conducted to investigate multi-material optimal topology depending on two cases of beam-column joint design within given crack information. It could be a new motivation for

design of structural retrofit in the near future.

Acknowledgments

This research was supported by a grant (NRF-2017R1A4A1015660) from NRF (National Research Foundation of Korea) funded by MEST (Ministry of Education and Science Technology) of Korean government.

References

- Abdel-Hafez, L.M., Abouelezz, A.E.Y. and Hassan, A.M. (2015), "Behavior of RC columns retrofitted with CFRP exposed to fire under axial load", *Hous. Build. Nat. Res. Center*, **11**, 68-81.
- ACI Committee 546-ACI 546R-04 (2004), Concrete Repair Guide; American Concrete Institute (ACI).
- Alam, A.M. (2014), "Effective Method of Repairing RC Beam Using Externally Bonded Steel Plate", *Appl. Mech. Mater.*, **567**, 399-404.
- Alonso, C., Ansola, R. and Querin, O.M. (2014), "Topology synthesis of multi-material compliant mechanisms with a sequential element rejection and admission method", *Finite Elem. Anal. Des.*, **85**, 11-19.
- Amin, N.M., Aziz, N.A., Joohari, I. and Alisibramulisi, A. (2016), "Retrofitting performance of reinforced concrete one way slab", *Jurnal Teknologi*, **78**, 41-45.
- Andra, P.H. and Maier, M. (1999), "Post strengthening of reinforced concrete structures by prestressed externally bonded carbon fibres reinforced polymer (CFRP) strips", *Proceedings of the Conference, 'Structural Faults and Repair 1999'*, London, UK.
- Anwar, G.A. and Versailot, P.D. (2016), "Effect of CFRP Retrofitting on Seismic Vulnerability of Reinforced Concrete Frame Structures in Pakistan", *Am. Sci. Res. J. Eng., Technol. Sci.*, **26**, 145-158.
- Asadpoure, A., Tootkaboni, M. and Valdevit, L. (2017), "Topology optimization of multiphase architected materials for energy dissipation", *Comput. Methods Appl. Mech. Eng.*, **325**(6), 314-329.
- Banh, T.T. and Lee, D.K. (2018a), "Topology optimization for thin plate on elastic foundations by using multi-material", *Steel Compos. Struct., Int. J.*, **27**(2), 177-184.
- Banh, T.T. and Lee, D.K. (2018b), "Multi-material topology optimization of Reissner-Mindlin plates using MITC4", *Steel Compos. Struct., Int. J.*, **27**(1), 27-33.
- Banh, T.T. and Lee, D.K. (2018c), "Multi-material topology optimization design for continuum structures with crack patterns", *Compos. Struct.*, **186**, 193-209.
- Bendsøe, M.P. and Kikuchi, N. (1988), "Generating optimal topologies in structural design using a homogenization method", *Computat. Methods Appl. Math.*, **71**(2), 197-224.
- Bendsøe, M.P. and Sigmund, O. (1999), "Material interpolation schemes in topology optimization", *Arch. Appl. Mech.*, **69**, 635-654.
- Bendsøe, M.P. and Sigmund, O. (2004), *Topology Optimization: Theory, Methods, and Applications*, SpringerVerlag Berlin Heidelberg, New York, NY, USA.
- Beres, A., El-Borgi, S., White, R.N. and Gergely, P. (1992), "Experimental results of repaired and retrofitted beam-column joint tests in lightly reinforced concrete frame buildings", Technical Rep. No.NCEER-92-0025; State University of New York at Buffalo, NY, USA.
- Blasques, J.P. and Stolpe, M. (2012), "Multi-material topology optimization of laminated composite beam cross sections", *Mater. Des.*, **94**(11), 3278-3289.
- Doan, Q.H. and Lee, D.K. (2017), "Optimum topology design of multi-material structures with non-spurious buckling constraints", *Adv. Eng. Software*, **114**, 110-120.
- Doan, H.D., Do, T.V., Pham, P.M. and Nguyen, D.D. (2017), "Validation simulation for free vibration and buckling of cracked Mindlin plates using phase-field method", *Mech. Adv. Mater. Struct.*, DOI: 10.1080/15376494.2018.1430262
- Gavali, V.C. and Kulkarni, H.B. (2018), "Mechanical and thermomechanical properties of carbon fibre reinforced thermoplastic composite fabricated using fused deposition modelling (fdm) method: a review", *Int. J. Mech. Product.*, **8**, 1161-1168.
- Gergely, J., Pantelides, C.P., Nuismer, R.J. and Reaveley, L.D. (1998), "Bridge pier retrofit using fiber-reinforced plastic composites", *J. Compos. Constr.*, **2-4**, 165-174.
- Hao, W., Liu, Y. and Fang, D. (2017), "Preparation and characterization of 3D printed continuous carbon fiber reinforced thermosetting composites", *Polym. Test.*, **65**, 29-34.
- International Concrete Repair Institute (2008), Guide for Surface Preparation for the Repair of Deteriorated Concrete Resulting From Reinforcing Steel Corrosion; Guideline No. 310.1R-2008 (formerly No. 03730).
- Kaiser, H.P. (1989), "Strengthening of reinforced concrete with epoxy-bonded carbon-fiber plastics", Doctoral Thesis; Diss. ETH, Nr.8918, ETH Zurich, Ch-8092 Zurich, Switzerland.
- Kim, Y., Ghannoum, W.M. and Jirsa, J.O. (2015), "Shear behaviour of full-scale reinforced concrete T-beams strengthened with CFRP strips and anchors", *Constr. Build. Mater.*, **94**, 1-9.
- Le, T.C., Phung, V.P., Thai, H.C., Nguyen, X.H. and Abdel, W.M. (2018), "Isogeometric analysis of functionally graded carbon nanotube reinforced composite nanoplates using modified couple stress theory", *Compos. Struct.*, **184**, 633-649.
- Lee, D.K. and Shin, S. (2015), "Optimizing structural topology patterns using regularization of Heaviside function", *Struct. Eng. Mech., Int. J.*, **55**(6), 1157-1176.
- Le-Trung, K., Lee, K., Shin, M. and Lee, J. (2011), "Analytical assessment and modeling of RC beam-column connections strengthen with CFRP composites", *Compos. Part B-Eng.*, **42**, 1786-1798.
- Lieu, X.Q. and Lee, J.H. (2017), "A multi-resolution approach for multi-material topology optimization based on isogeometric analysis", *Comput. Methods Appl. Mech. Eng.*, **323**, 272-302.
- Lieu, X.Q., Lee, S.H., Kang, J.W. and Lee, J.H. (2018a), "Bending and free vibration analyses of in-plane bi-directional functionally graded plates with variable thickness using isogeometric analysis", *Compos. Struct.*, **192**, 434-451.
- Lieu, X.Q., Lee, J.W., Lee, D.K., Kim, D.H., Lee, S.H. and Lee, J.H. (2018b), "Shape and size optimization of functionally graded sandwich plates using isogeometric analysis and adaptive hybrid evolutionary firefly algorithm", *Thin-Wall. Struct.*, **124**, 588-604.
- Maria, T.D.R. (2016), "Role of beam-column joints in the seismic response of non-conforming RC frames", *IV Workshop on New Boundaries of Structural Concrete (NBSC2016)*, Anacapri, Italy.
- Masuelli, M.A. (2013), "Introduction of Fiber-Reinforced Polymers and Composites: Concepts, Properties and Process", 1-24, InTech, Croatia, pp. 1-24.
- Nguyen, D.D. and Do, N. (2014), "Nonlinear stability analysis of imperfect three-phase polymer composite plates in thermal environments", *Compos. Struct.*, **109**, 130-138.
- Nguyen, D.D., Tran, Q.Q. and Do, N. (2013), "A nonlinear stability analysis of imperfect three-phase polymer composite plates", *Mech. Compos. Mater.*, **49**, 345-358.
- Nguyen, D.D., Tran, Q.Q. and Nguyen, D.K. (2017a), "New approach to investigate nonlinear dynamic response and

- vibration of imperfect functionally graded carbon nanotube reinforced composite double curved shallow shells subjected to blast load and temperature”, *Aerosp. Sci. Technol.*, **71**, 360-372.
- Nguyen, D.D., Lee, J.H., Nguyen, T.T. and Pham, T.T. (2017b), “Static response and free vibration of functionally graded carbon nanotube-reinforced composite rectangular plates resting on Winkler–Pasternak elastic foundations”, *Aerosp. Sci. Technol.*, **68**, 391-402.
- Nguyen, D.D. and Pham, D.N. (2017c), “The dynamic response and vibration of functionally graded carbon nanotubes reinforced composite (FG-CNTRC) truncated conical shells resting on elastic foundation”, *Mater. Special Issue “Adv. Compos.”*, **10**(10), 1194.
- Pham, V.T. and Nguyen, D.D. (2016), “Non-linear dynamic response and vibration of an imperfect three-phase laminated nanocomposite cylindrical panel resting on elastic foundations in thermal environments”, *Sci. Eng. Compos. Mater.*, **24**(6), 951-962.
- Pham, P.M., Do, V.T., Doan, H.D. and Nguyen, D.D. (2018), “The stability of cracked rectangular plate with variable thickness using phase field method”, *Thin-Wall. Struct.*, **129**, 157-165.
- Phung, V.P., Abdel, W.M., Liew, K.M., Bordas, S.P.A., Nguyen, X.H. (2015), “Isogeometric analysis of functionally graded carbon nanotube-reinforced composite plates using higher-order shear deformation theory”, *Compos. Struct.*, **123**, 137-149.
- Phung, V.P., Abdel, W.M., Lieu, X.Q., Nguyen, X.H. (2017a), “Size-dependent isogeometric analysis of functionally graded carbon nanotube-reinforced composite nanoplates”, *Compos. Struct.*, **166**, 120-135.
- Phung, V.P., Ferreira, A.J.M., Nguyen, X.H., Abdel, W.M. (2017b), “An isogeometric approach for size dependent geometrically nonlinear transient analysis of functionally graded nanoplates”, *Compos. Part B: Eng.*, **118**, 125-134.
- Phung, V.P., Abdel, W.M., Le, T.C., Nguyen, X.H. (2018), “Nonlinear transient isogeometric analysis of FG-CNTRC nanoplates in thermal environments”, *Compos. Struct.*, **201**, 882-892.
- Shahri, M.B. and Moeenfard, H. (2018), “Topology optimization of fundamental compliant mechanisms using a novel asymmetric beam flexure”, *Int. J. Mech. Sci.*, **135**, 383-397.
- Shobeiri, V. (2015), “The topology optimization design for cracked structures”, *Eng. Anal. Boundary Elem.*, **58**, 26-38.
- Song, L. and Yu, Z. (2015), “Fatigue performance of corroded reinforced concrete beams strengthened with CFRP sheets”, *Constr. Build. Mater.*, **90**, 99-109.
- Tavakoli, R. and Mohseni, S.M. (2014), “Alternating active-phase algorithm for multimaterial topology optimization problems: a 115-line matlab implementation”, *Struct. Multidiscipl. Optimiz.*, **49**, 621-642.
- Truong, G.T. and Choi, K.K. (2017), “Seismic Performance of Exterior RC Beam–Column Joints Retrofitted using Various Retrofit Solutions”, *Int. J. Concrete Struct. Mater.*, **11**, 415-433.
- Woischwill, C. and Kim, I.Y. (2018), “Multimaterial multijoint topology optimization”, *Int. J. Numer. Methods Eng.*, **115**(13), 1552-1579. DOI: 10.1002/nme.5908
- Xia, Q. and Wang, M.Y. (2008), “Topology optimization of thermoelastic structures using level set method”, *Computat. Mech.*, **42**(6), 837.
- Zhou, W.D. and Chen, J.S. (2018), “3D Printing of Carbon Fiber Reinforced Plastics and their Applications”, *Mater. Sci. Forum*, **913**, 558-563.
- Zhou, S. and Wang, M. (2006), “Multimaterial structural topology optimization with a generalized Cahn-Hilliard model of multiphase transition”, *Struct. Multidiscipl. Optimiz.*, **33**(2), 89-111.